Magnetic Properties of Nanocrystalline CoW Thin Film Alloys Electrodeposited from Citrate Baths

Doek-Yong Park and Jang-Myoun Ko*

Department of Applied Materials Engineering
*Department of Chemical Technology
Hanbat National University, San 16-1, Dukmyung-dong, Yuseong-gu, Daejeon, 305-719, Republic of Korea

Abstract: Magnetic CoW thin film alloys were electrodeposited from citrate baths to investigate the resulting microstructure and magnetic properties. Deposit tungsten (W) content in the films electrodeposited at 70°C were independent of current density, while coercivity decreased from hard ($H_{C//}$ ~150 Oe and $H_{C\perp}$ ~240 Oe) to soft magnetic properties ($H_{C//}$ ~20 Oe and $H_{C\perp}$ ~30 Oe) with increasing current densities from 10 to 100 $mA \cdot cm^{-2}$, with deposit W content (~40%) relatively unaffected by the applied current density. X-ray diffraction analysis indicated that hcp Co_3W phases [(200), (201) and (220) planes] in the CoW films electrodeposited at 70°C and 10 $mA \cdot cm^{-2}$ were dominant, whereas amorphous CoW phases with small amount of hcp Co_3W [(002) planes] were dominant with deposition at 70°C and 100 $mA \cdot cm^{-2}$. At intermediate current densities (25 and 50 $mA \cdot cm^{-2}$), hcp Co_3W phases [(200), (002), (201) and (220)] were observed. The average grain size was measured to be 30 nm from Sherrer formula. It is suggested that the change of the deposit coercivities in the CoW thin films electrodeposited at 70°C is attributed to the change of microstructures with varying the current density. Nanostructured Co_3W/amorphous-CoW multilayers were fabricated by alternating current density between 10 and 100 $mA \cdot cm^{-2}$, varying the individual layer thickness. The magnetic properties of Co_3W/amorphous-CoW multilayers were strongly dependent on the thickness of the alternating hard and soft magnetic thin films. The nanostructured Co_3W/amorphous-CoW multilayers exhibited a shift from low to high coercivities suggesting a strong coupling effect.

Key words : CoW alloy, Magnetic properties, Electrodeposition, Citrate bath, Nanocrystalline

1. Introduction

Tungsten and tungsten alloys are technologically and economically important. Of all the metals, tungsten possesses the highest melting point (3410°C), the lowest coefficient of linear thermal expansion (4.3 × 10^{-6}/°C), the highest tensile strength (4.0 MPa) and, the highest Youngs modulus of elasticity (34 GPa), high thermal conductivity (210 $W \cdot m^{-1} \cdot K^{-1}$), and one of the highest densities of all metals (19.3 g/cm^3)[1]. However, the high melting temperature of tungsten makes the preparation and processing of tungsten alloys very difficult. There are various methods to make tungsten alloys such as powder metallurgy, chemical vapor deposition and electrodeposition[2]. Electrodeposition and electroless deposition have many advantages over another process: low cost, easy scale up and maintenance, low operating temperatures, and the ability to "tailor" deposit structure and properties[3,4].

Since Fink and Jones had first electrodeposited tungsten alloys from a solution containing sodium carbonate and sodium tungstate in 1931[5]. It is well known that tungsten cannot be electrodeposited alone from an aqueous solution, but only in conjunction with deposition of other metals, known as induced codeposition[1]. Many researchers had studied the electrodeposition process of tungsten with iron-group (cobalt, nickel and iron) metals from aqueous solutions[6-8]. Among tungsten alloys, electrodeposited magnetic CoW thin film alloys have been investigated with potential applications in computer read/write heads[9-10], microelectromechanical systems (MEMS)[11-13] and ultra large scale integration (ULSI) devices[14-15] because of favorable magnetic properties combined with wear resist-ance, corrosion resistance, and good lubrication properties[16-17]. Tungsten forms hard alloys with cobalt, retaining some of its unusual properties such as magnetic, highest tensile strength, electrochemical and high corrosion resistance. Therefore, the electrodeposition of tungsten alloys has become a subject of pronounced practical significance[18].

Although several researchers have studied the magnetic properties of CoW thin film alloys with respect to the relationship between electrodeposition parameters and their magnetic properties[16,19-20]. However, these relationships are not understood clearly. It is the purpose of the present work to study the effects of electrodeposition parameters (mainly current density) on the microstructure and the resulting magnetic properties of CoW thin films electrodeposited from citrate baths.

2. Experimental

Solution compositions are listed in Table 1. Ammonium

†E-mail: jmko@hanbat.ac.kr

237

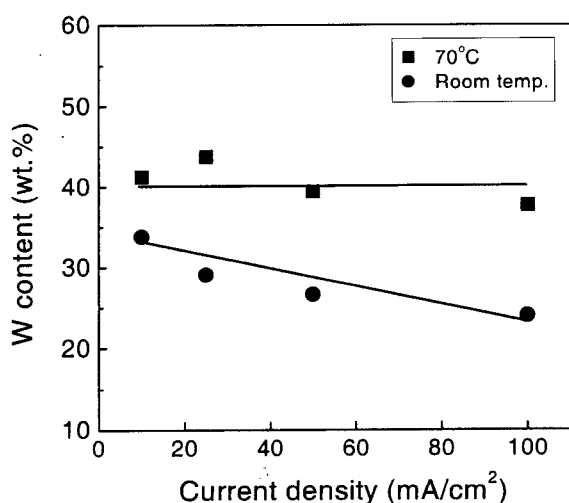## Table 1. Bath composition for CoW electrodeposits.

Chemical/conditions	Concentration(M)
$CoCl_2 \cdot 6H_2O$	0.126
$Na_2WO_4 \cdot 2H_2O$	0.041
$(NH_4)_2 \cdot H \cdot C_6H_5O_7$	0.33
NH_4Cl	0.93
pH	8.7

citrate, $(NH_4)_2 \cdot H \cdot C_6H_8O_7$, was used as complex agent to prevent the precipitation of the metallic ions in electroplating baths at pH = 8.5. NH_4Cl was used as supporting electrolyte. Solutions were exposed to air and solution pH was adjusted by adding NH_4OH or HCl; experiments were conducted at pH 8.7 and 60 coulombs/cm². Current densities varied from 10 to 100 mA/cm² and electrodeposition was carried out at room temperature and 70°C without stirring. CoW thin films were electrodeposited on brass substrates; cobalt sheet was used as soluble anode.

Deposit Co contents were analyzed using atomic absorption spectroscopy (AA) (Model 280, Perkin-Elmer); deposit W contents were analyzed using energy dispersive spectroscopy (EDS) (Kevex Inc.). Magnetic properties, such as coercivity (H_C), squareness ($S = M_r/M_S$) and M_s, were determined using a vibrating sample magnetometer (Model 880, ADE technologies Inc.). X-ray diffractometer (XRD) (Model 42202, Norelco, North American Phillips Company Inc.) with Cu K_α radiation was used to identify the phases and to determine grain size. Conditions of XRD were a scanning range (20°-100°) with 0.03° increments and a one second dwell time.

3. Results and Discussion

Fig. 1 shows the dependence of deposit W content on current density and deposition temperature in the electrodeposited CoW thin films. The deposit W content in CoW films electrodeposited at room temperature decreased from ~34 to ~24wt.%. However, The deposit W content (~40 wt.%) in CoW films electrodeposited at 70°C was independent of current density with varying current density from 10 to 100 mA/cm². The CoW thin film alloys deposited at 70°C exhibited higher deposit W content than that of CoW films deposited at room temperature. The cathode current efficiency with increasing current density slightly decreased from ~10% to ~7% with electrodeposition at room temperature as shown in Fig. 2; current efficiency also decreased from ~27 to ~12% with electrodeposition at 70°C. Frantsevich-Zabludovskaya and Zayats[21] reported that the W content and the faradic efficiency in CoW alloys obtained from ammoniacal citrate baths increased with increasing electrodeposition temperature. Also, Hoar and Bucklow[22] reported that the applied current density influences the current efficiency and the current efficiency decreased with increasing current density in CoW alloys. Fig. 3 shows the dependence of current efficiency of the CoW thin film alloys electrodeposited at 70°C and two different current densities (10 and 100 mA/cm²) on film thickness. The current efficiency was independent of film thickness (~20%) with electrodeposition at 100 mA/cm², whereas the current efficiency of the CoW films electrodeposited at 10 mA/cm² decreased from ~50% to ~25%. The above results indicate that the higher current efficiency was obtained at higher temperature, low current density, and thinner film thickness.

Fig. 4 shows the dependence of coercivity of the CoW thin film alloys electrodeposited at room temperature and 70°C on the current density. Parallel coercivities of the CoW thin films electrodeposited at room temperature exhibited soft magnetic property ($H_{C//}$ ~20 Oe) and remained fairly constant with increasing current density, while perpendicular coercivity ($H_{C\perp}$) decreased from ~230 to ~130 Oe. Parallel coercivities of the CoW thin films electrodeposited at 70°C decreased from ~150 to ~20 Oe; perpendicular coercivities decreased

Fig. 1. Dependence of deposit W content of the CoW thin film alloys electrodeposited at room temperature and 70°C on current density.
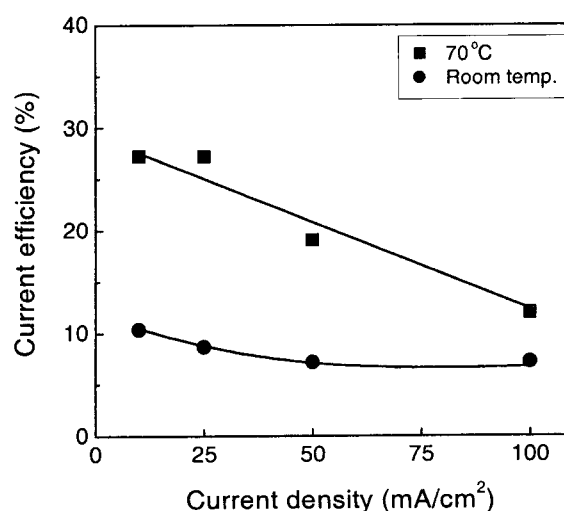
Fig. 2. Dependence of current efficiencies of the CoW thin film alloys electrodeposited at room temperature and 70°C on current density.
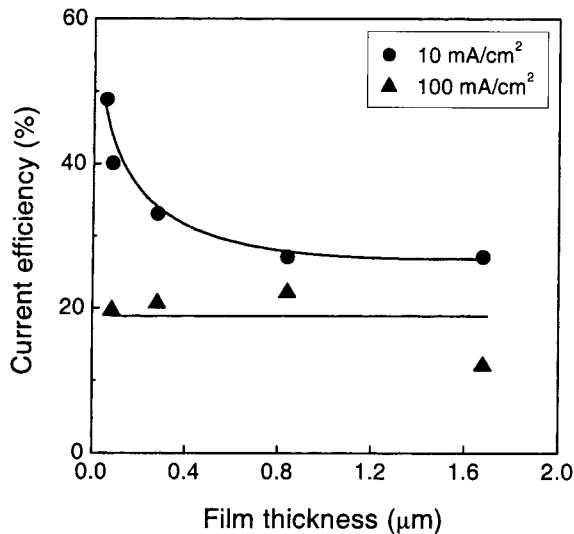
Fig. 3. Dependence of current efficiencies of the CoW thin film alloys electrodeposited at 70°C on film thickness.
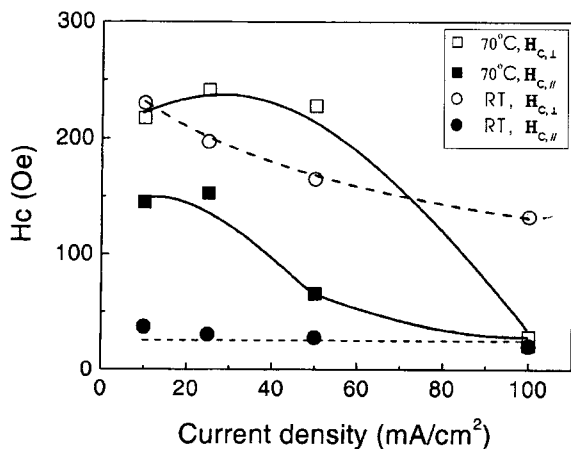

Fig. 4. Dependence of coercivity of the CoW thin film alloys electrodeposited at room temperature and 70°C on film thickness.

from hard magnetic ($H_{C,\perp}$ ~240 Oe) to soft magnetic properties ($H_{C,//}$ ~30 Oe). Parallel squareness of CoW thin films electrodeposited at room temperature was measured to be in the ranges between 0.64 and 0.51 with increasing current density, whereas parallel squareness of CoW thin films electrodeposited at 70°C decreased from 0.48 to 0.17. The parallel B-H hysteresis loops of CoW thin films electrodeposited at room temperature and 70°C with increasing current density are shown in Fig. 6. The CoW thin film alloys electrodeposited at 70°C show a transition from soft ($H_{C,//}$ ~20 Oe) to hard ($H_{C,//}$ ~150 Oe) magnetic properties as current density decreased from 100 to 10 mA/cm^2, whereas the CoW deposits electrodeposited at room temperature exhibited soft magnetic properties ($H_{C,//}$ ~20 Oe at 100 mA/cm^2 and $H_{C,//}$ ~30 Oe at 10 mA/cm^2).

XRD patterns of CoW deposits resulting from the change of current densities are shown in Fig. 7. XRD analysis indicates that the CoW thin films deposited at room temperature
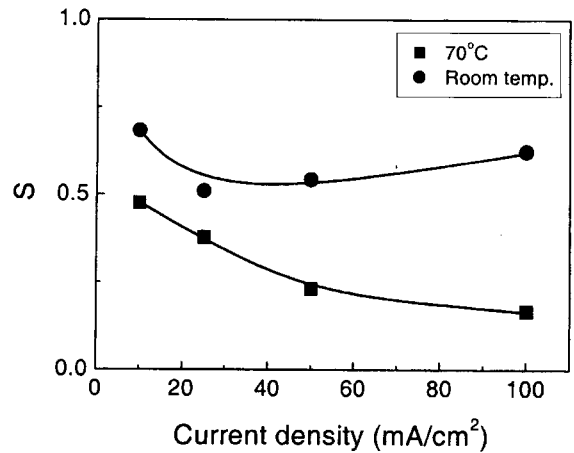

Fig. 5. Dependence of squareness (parallel) of the CoW thin film alloys electrodeposited at room temperature and 70°C on film thickness.

with current densities of 10, 25 and 100 mA/cm^2 consist of hcp Co$_3$W structure [(200), (002) and (201) phases]. The intensity of those phases is relatively low. The average grain size of those phases was calculated to be ~28 nm using the Sherrer formula. On the other hand, the CoW thin films deposited at 50 mA/cm^2 has amorphous phases from the XRD analysis. It is observed that the CoW thin films electrodeposited at 70°C exhibited the hcp Co$_3$W structures [(200), (002), (201) and (220) planes] as current densities decreased from 100 to 10 mA/cm^2. The intensity of those phases is relatively higher than those of the CoW thin films deposited at room temperature. The average grain size was measured to be ~30 nm. The CoW films electrodeposited at 100 mA/cm^2 mainly consist of amorphous phases because of very small amount of hcp Co$_3$W peaks [(002) phases], whereas the development of hcp Co$_3$W peaks with (200), (002), (201) and (220) planes was observed with electrodeposition at 50, 25 and 10 mA/cm^2. From the XRD analysis, it is believed that the changes of magnetic properties from soft ($H_{C,//}$ ~20 Oe and $H_{C,\perp}$ ~30 Oe, at 100mA/cm^2) to hard ($H_{C,//}$ ~150 Oe and $H_{C,\perp}$ ~240 Oe, at 10 mA/cm^2) in the CoW films deposited at 70°C may be attributed to the change of the microstructures of the films. Park et al. reported that the addition of phosphorus into CoNi deposits from chloride baths resulted in the increase of hcp structure with preferred (002) planes. They suggested the coercivity enhancement is closely related to the formation (intensity) of hcp (002) planes in CoNiP deposits[3]. Homma et al. reported that the electroless CoNiP deposits from sulfate baths consisted of a mixture of <002> perpendicularly oriented hcp regions and randomly oriented fcc regions, and that an increase in hcp regions produced higher $H_{C,\perp}$ deposits[23]. They also suggested that the coercivity of electroless CoNiP deposits is directly related to the size and orientation of the crystallites. Naoe et al. also reported that the decrease of coercivity in Co$_{100-x}$W$_x$ (13 × 25) films deposited by rf diode sputtering because of the structural changes from crystalline to amorphous[19].
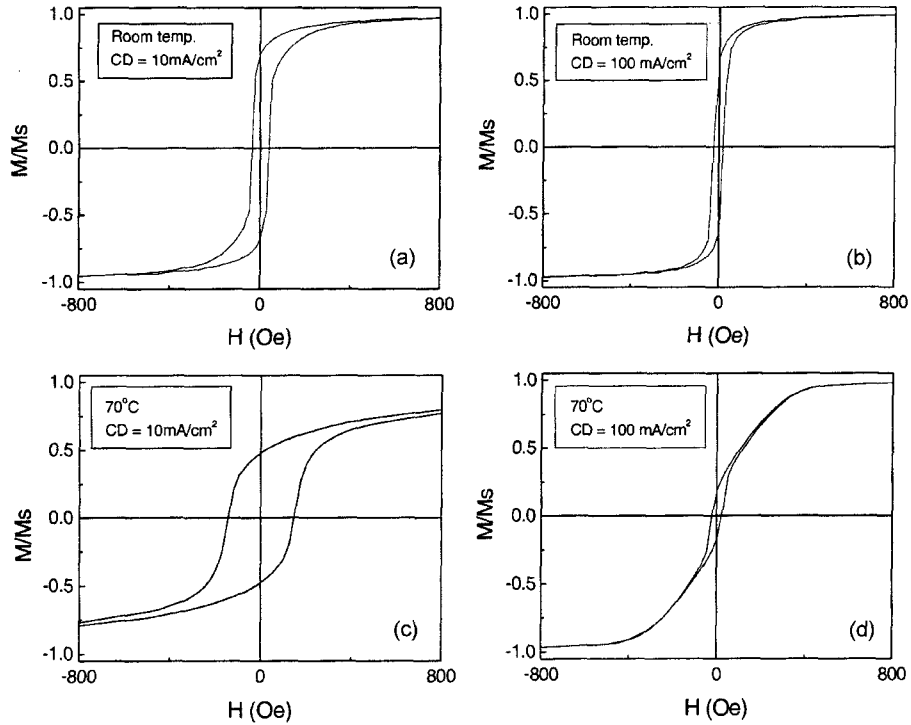
Fig. 6. Dependence of parallel B-H loop of the CoW thin film alloys electrodeposited at room temperature and 70°C on current density.
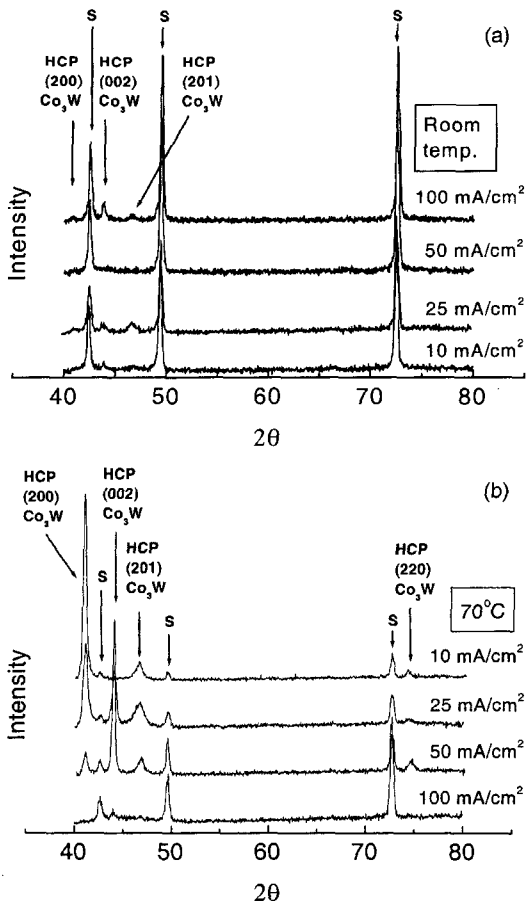

Fig. 7. XRD patterns of CoW thin film electrodeposited with various current densities at (a) room temperature and (b) 70°C.
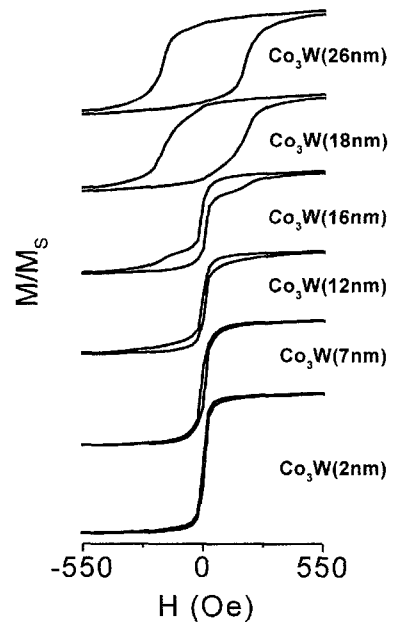

Fig. 8. B-H loops obtained from the alternative multilayers of CoW thin films consisting of CoW layers deposited at 100 mA/cm² with a fixed 30 nm thick and a varied Co₃W layer electrodeposited at 100 mA/cm² with thickness from 2 nm to 26 nm.

From the above results, it should be interesting to fabricate the nanostructured multilayers by alternatively changing the current densities between 10 and 100 mA/cm², with variation of individual layer thickness and to investigate their magnetic properties. Fig. 8 shows the magnetic B-H hysteresis loops obtained from the alternative multilayers. The layer thickness
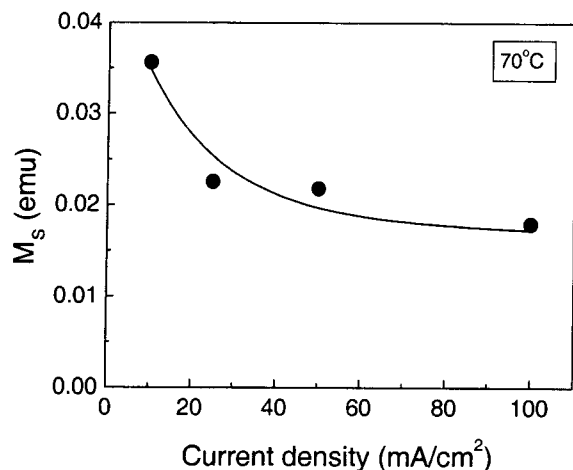
Fig. 9. Dependence of magnetization of the CoW thin film alloys electrodeposited at 70°C on current density.

of CoW thin film, which mainly consists of amorphous phases (called as amorphous CoW layer unless otherwise noted), electrodeposited at 100 mA/cm² (Fig. 7b) was fixed 30 nm thick; whereas the layer thickness of CoW thin film electrodeposited at 10 mA/cm² which consist of hcp Co₃W phases [(200), (201) and (220) planes] was varied from 2 nm to 26 nm. It is observed that the degree of magnetic hysteresis increases with increasing the layer thickness of hcp Co₃W phases (electrodeposited at 10 mA/cm²). Magnetic properties of alternative Co₃W/amorphous-CoW multilayers were strongly dependent on alternative film thickness and portion of hard (deposited at 10 mA/cm²) and soft (deposited at 10 mA/cm²) magnetic films. The Co₃W/amorphous-CoW multilayers showed a gradual transition from soft ($H_{C,//}$ ~3 Oe) to hard magnetic ($H_{C,//}$ ~250 Oe) properties with increasing the portion of hcp Co₃W phases deposited at 10 mA · cm⁻², suggesting there is a strong coupling effect between multilayers[19]. Fig. 9 shows the dependence of magnetization of CoW thin film alloys electrodeposited at 70°C on current density. The saturation magnetization decreased with increasing current density due to lower current efficiency. This is in agreement with the trend observed in current efficiency data, as shown in Fig. 2. It is interesting to notice that the degree of the hysteresis of magnetization loop decrease with increasing electrodeposition current density from 10 mA/cm² to 100 mA/cm², indicating that magnetic properties of CoW thin film alloys is changed from hard ($H_{C,//}$ = 150 Oe) to soft ($H_{C,//}$ = 20 Oe). Such a decrease in parallel coercivity ($H_{C,//}$) may be attributed to the structural change of the films.

4. Conclusions

Magnetic CoW thin film alloys were electrodeposited from citrate baths to investigate the dependence of magnetic properties on the microstructure. Current efficiencies were affected by the deposit temperature and deposit film thickness. The microstructure of the film and magnetic properties

of CoW thin film alloys strongly were influenced by the current density and deposit temperature. Deposit W content (~40 wt.%) in the CoW films electrodeposited at 70°C was independent of current density. On the other hand, deposit W content decreased from 34wt.% to 24wt.% in the CoW films electrodeposited at room temperature with varying current densities. The higher current efficiency was obtained at higher deposit temperature, low current density, and thinner film thickness.

It is suggested that the changes of magnetic properties from soft ($H_{C,//}$ ~20 Oe and $H_{C,\perp}$ ~30 Oe, at 100 mA/cm²) to hard ($H_{C,//}$ ~150 Oe and $H_{C,\perp}$ ~240 Oe, at 10 mA/cm²) in the CoW films deposited at 70°C may be attributed to the change of the microstructures of the film. Because the CoW thin film alloy deposited at 100 mA/cm² and 70°C mainly consists of amorphous phases, whereas the CoW thin film alloy deposited at 10 mA/cm² and 70°C exhibited the prominent development of various hcp phases [(200), (002), (201) and (220) planes]. The Co₃W/amorphous-CoW multilayers electrodeposited at 70°C exhibited a transition from soft to hard magnetic properties with increasing the portion of hcp Co₃W phases, suggesting a strong coupling effect between multilayers.

References

1. O. Younes and E. Gileadi, *J. Electrochem. Soc.* **149** (2002) C100.
2. A. Crowson and E.S. Chen, *JOM*, **43** (1991) 27.
3. D.-Y. Park, N. V. Myung, M. Schwartz, and K. Nobe, *Electrochim. Acta*, **47** (2002) 2893.
4. M. Donten, T. Gromulski, and Z. Stojek, *J. Alloys and Compounds*, **279** (1998) 272.
5. C. G. Fink and F. L. Jones, *Trans. Electrochem. Soc.* **59** (1931) 461.
6. A. Brenner, Electrodeposition of Alloys, Vol. 2, Academic Press, New York, NY, 1963, p. 589.
7. S. M. Mayanna, N. Nunichandraiah, and T. Mimani, *J. Appl. Electrochem.* **23** (1993) 339.
8. S. M. Mayanna and T. Mimani, *Surf. Coat. Technol.* **79** (1996) 246.
9. A. Chiu, I. Croll, D. E. Heim, R. E. Jones, Jr., P. Kasiraj, K.B. Klassen, and C. D. R. G. Simmons, *IBM J. Res. Develop*, **40** (1996) 283.
10. P. C. Andricacos and N. Robertson, *IBM J. Res. Develop*, **42** (1998) 671.
11. E. J. OSullivan, E. I. Cooper, L. T. Romankiw, K. T. Kwietniak, P. L. Trouilloud, J. Horkans, C. V. Jahnes, I. V. Babich, S. Krongelb, S. C. Hegde, J. A. Tornello, N. C. LaBianca, J. M. Cotte, and T. J. Chainer, *IBM J. Res. Develop*, **42** (1998) 681.
12. C. Liu, T. Tsao, G.-B. Lee, J. T. S. Leu, Y. W. Yi, Y.-C. Tai, and C.-M. Ho, *Sensors and Actuators* **78** (1999) 190.
13. F. E. Rasmussen, J. T. Ravnkilde, P. T. Tang, O. Hansen, and S. Bouwstra, *Sensors and Actuators A*, **92** (2001) 242.
14. A. Kohn, M. Eizenberg, Y. Shacham-Diamand, B. Israel, and Y. Sverdlov, *Microelectronic Eng.* **55** (2001) 297.

15. A. Kohn, M. Eizenberg, Y. Shacham-Diamand, and Y. Sverdlov, *Mater. Sci. Eng.* A**302** (2001) 18.

16. V. G. Shadrow, A. V. Boltushkin, T. A. Tochitskii, and L. B. Sosnovskaja, *Thin Solid Films*, **202** (1991) 61.

17. U. Admon, M. P. Dariel, and E.Grunbaum, *J. Appl. Phys.* **59** (1986) 2002.

18. Z. A. Hamid, *Mater. Lett.* **57** (2003) 2558.

19. M. Naoe, H. Kazama, Y. Hoshi, and S. Yamanaka, *J. Appl. Phys.* **53** (1982) 7846.

20. M. Svensson, U. Wahlstöm, and G. Holmbom, *Surf. Coat. Tech.* **105** (1998) 218.

21. T. F. Frantsevich-Zabludovskaya and A.I. Zayats, *Zh. Prikl.Khim.* **30** (1957) 723.

22. T. P. Hoar and I. A. Bucklow, *Trans. Inst. Met. Finish.* **32** (1955) 186.

23. T. Homma, K. Inoue, H. Asai, K. Ohrui, T. Osaka, Y. Yamazaki, and T. Namikawa, *IEEE Trans. J. Magn. Jpn.* **6** (9) (1991) 758.